Geochemistry Geophysics Geosystems G3

Technical Brief
Volume 12, Number 3
1 March 2011
Q03001, doi:10.1029/2010GC003322
ISSN: 1525-2027

Published by AGU and the Geochemical Society

In situ δ^7Li, Li/Ca, and Mg/Ca analyses of synthetic aragonites

R. I. Gabitov
Department of Earth and Space Sciences, University of California, Los Angeles, California 90095, USA (gabitr@ucla.edu)

Formerly at Department of Geology and Geophysics, Woods Hole Oceanographic Institution, Woods Hole, Massachusetts 02543, USA

Formerly at Department of Earth and Environmental Sciences, Rensselaer Polytechnic Institute, Troy, New York 12180, USA

A. K. Schmitt
Department of Earth and Space Sciences, University of California, Los Angeles, California 90095, USA

M. Rosner
Department of Geology and Geophysics, Woods Hole Oceanographic Institution, Woods Hole, Massachusetts 02543, USA

Also at Division I.1, Analytical Chemistry; Reference Materials, BAM Federal Institute for Materials Research and Testing, Unter den Eichen 87, D-12205 Berlin, Germany

Also at Section 4.2: Inorganic and Isotope Geochemistry, Deutsches GeoForschungsZentrum, Telegrafenberg, D-14473 Potsdam, Germany

K. D. McKeegan
Department of Earth and Space Sciences, University of California, Los Angeles, California 90095, USA

G. A. Gaetani and A. L. Cohen
Department of Geology and Geophysics, Woods Hole Oceanographic Institution, Woods Hole, Massachusetts 02543, USA

E. B. Watson
Department of Earth and Environmental Sciences, Rensselaer Polytechnic Institute, Troy, New York 12180, USA

T. M. Harrison
Department of Earth and Space Sciences, University of California, Los Angeles, California 90095, USA

[1] In situ secondary ion mass spectrometry (SIMS) analyses of δ^7Li, Li/Ca, and Mg/Ca were performed on five synthetic aragonite samples precipitated from seawater at 25°C at different rates. The compositions of δ^7Li in bulk aragonites and experimental fluids were measured by multicollector inductively coupled plasma–mass spectrometry (MC-ICP-MS). Both techniques yielded similar δ^7Li in aragonite when SIMS

analyses were corrected to calcium carbonate reference materials. Fractionation factors $\alpha^7Li/^6Li$ range from 0.9895 to 0.9923, which translates to a fractionation between aragonite and fluid from −10.5‰ to −7.7‰. The within-sample δ^7Li range determined by SIMS is up to 27‰, exceeding the difference between bulk δ^7Li analyses of different aragonite precipitates. Moreover, the centers of aragonite hemispherical bundles (spherulites) are enriched in Li/Ca and Mg/Ca relative to spherulite fibers by up to factors of 2 and 8, respectively. The Li/Ca and Mg/Ca ratios of spherulite fibers increase with aragonite precipitation rate. These results suggest that precipitation rate is a potentially important consideration when using Li isotopes and elemental ratios in natural carbonates as a proxy for seawater composition and temperature.

Components: 8800 words, 7 figures, 5 tables.

Keywords: lithium; isotope; aragonite; rate; SIMS; magnesium.

Index Terms: 1041 Geochemistry: Stable isotope geochemistry (0454, 4870); 4924 Paleoceanography: Geochemical tracers; 3630 Mineralogy and Petrology: Experimental mineralogy and petrology.

Received 10 August 2010; **Revised** 30 November 2010; **Accepted** 4 January 2011; **Published** 1 March 2011.

Gabitov, R. I., A. K. Schmitt, M. Rosner, K. D. McKeegan, G. A. Gaetani, A. L. Cohen, E. B. Watson, and T. M. Harrison (2011), In situ δ^7Li, Li/Ca, and Mg/Ca analyses of synthetic aragonites, *Geochem. Geophys. Geosyst.*, *12*, Q03001, doi:10.1029/2010GC003322.

1. Introduction

[2] The fractionation of trace elements and isotopes during precipitation of carbonate minerals in the oceanic environment is the basic tool used for reconstruction of the history of oceanographic variability through time. While not a significant Li sink, marine carbonates are known to be good recorders of seawater Li abundance (~180 ppb) and δ^7Li (~+33‰) [*Morozov*, 1968; *Ronov et al.*, 1970; *Delaney et al.*, 1985; *Hall et al.*, 2005]. Lithium isotopic composition is typically expressed as

$$\delta^7Li = \frac{\left(^7Li/^6Li\right)_{sample} - \left(^7Li/^6Li\right)_{LSVEC}}{\left(^7Li/^6Li\right)_{LSVEC}} \cdot 10^3‰$$

where the NIST SRM 8545 (LSVEC) lithium carbonate is the certified isotope reference material which defines the zero point on the δ^7Li scale. Lithium enters the ocean through river input (discharge weighted average of the major world rivers δ^7Li ≈ + 23‰) and hydrothermal marine fluids (average δ^7Li ≈ +7‰) [*Chan et al.*, 1993, 1994; *Huh et al.*, 1998; *Coplen et al.*, 2002; *White*, 2005]. Therefore, the changes of seawater Li and δ^7Li should reflect changes in continental weathering environment (δ^7Li in continental rocks varies from −10‰ to +19‰) and hydrothermal input over geological time [*Tomascak*, 2004]. Lithium is removed from the ocean by reaction with oceanic crust and absorption on surfaces of mineral particles. These Li input and output processes fractionate δ^7Li between solid and fluid phases with preferential incorporation of ^{7}Li into solution. Hence, riverine δ^7Li inputs depend not only on the geologic settings but also on the weathering rate of continental rocks.

[3] No relationship between δ^7Li and temperature has been found in synthetic calcite, foraminifera, or corals described in the studies of *Marriott et al.* [2004a], *Hall et al.* [2005], and *Rollion-Bard et al.* [2009]. This supports the potential for these Ca carbonate minerals to be a proxy for continental weathering and hydrothermal activity in the ocean. However, no experimental work has been performed to evaluate the influence of growth rate on Li isotope fractionation and Li partitioning between calcium carbonate minerals and fluid.

[4] It has been shown, however, that Li/Ca in foraminifera calcite depends on the saturation state of seawater (Ω), which is linked to mineral growth rate [*Hall and Chan*, 2004; *Bryan and Marchitto*, 2008]. Further, there is a negative correlation between temperature and the Li/Ca ratio of calcitic forams, calcitic brachiopods, and aragonitic corals at 2 to 28°C [*Delaney et al.*, 1989; *Marriott et al.*, 2004a; *Hall and Chan*, 2004; *Bryan and Marchitto*, 2008; *Case et al.*, 2010; *Hathorne et al.*, 2009; *Montagna et al.*, 2009]. An experimental study of Li/Ca in calcite confirms the observed natural trend, i.e., Li/Ca partition coefficient $\left(K_d^{Li/Ca} = \frac{(Li/Ca)_{solid}}{(Li/Ca)_{fluid}}\right)$

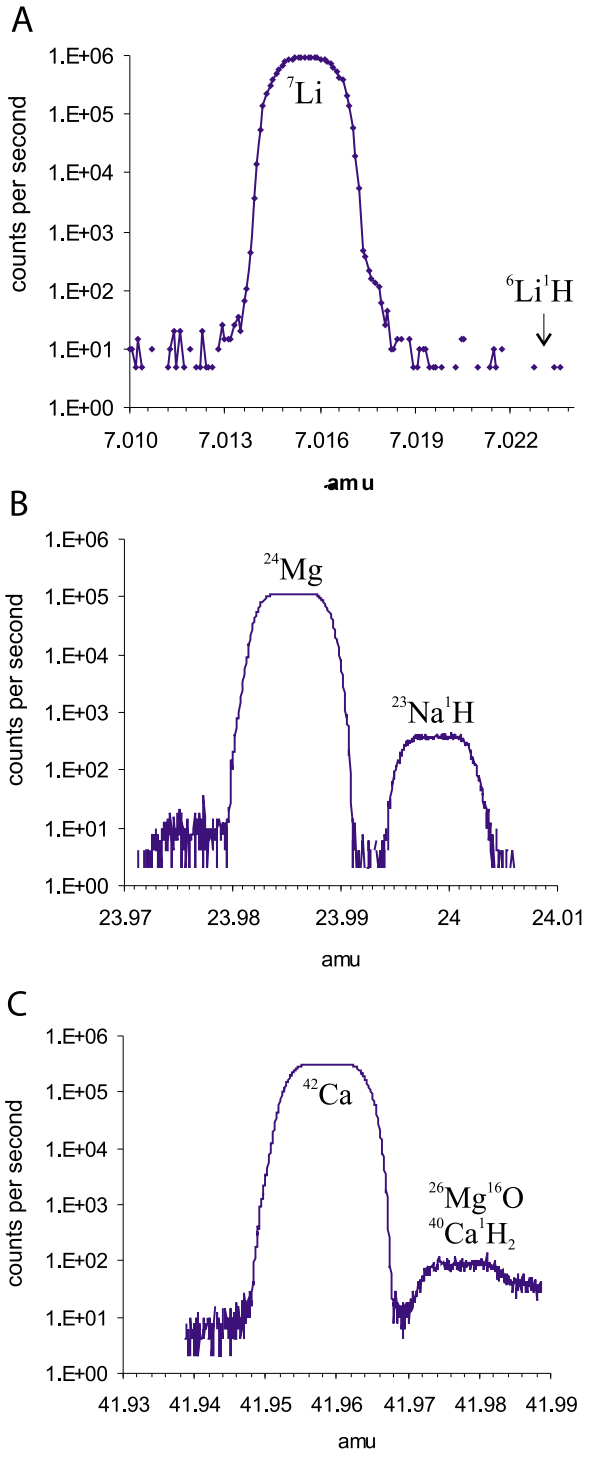

Figure 1. High-resolution scans of positive ion species of (a) ^{7}Li, (b) ^{24}Mg, and (c) ^{42}Ca at MRP ≈ 2900 with the mass of interest and resolved molecular interferences identified. ^{6}Li^{1}H was not detected at the relevant mass offset (0.0069 amu) from the ^{7}Li peak (Figure 1a). We tentatively identify a resolved interference at higher mass relative to ^{24}Mg as ^{23}Na^{1}H (Figure 1b) and to ^{42}Ca as ^{26}Mg^{16}O and ^{40}Ca^{1}H$_2$ (Figure 1c).

between solid and fluid phase decreases with increasing temperature from 5 to 30°C [*Marriott et al.*, 2004a]. However, temperature is not the only factor responsible for Li/Ca and Mg/Ca variation in corals. Several studies have reported that Mg/Ca (and, to a lesser extent, Li/Ca) is enriched in the coral centers of calcification (COC) relative to the fibrous material [*Meibom et al.*, 2004, 2006; *Sinclair et al.*, 2006; *Gagnon et al.*, 2007; *Rollion-Bard et al.*, 2009; *Case et al.*, 2010]. Therefore, the influence of crystallization kinetics on Li/Ca and Mg/Ca need

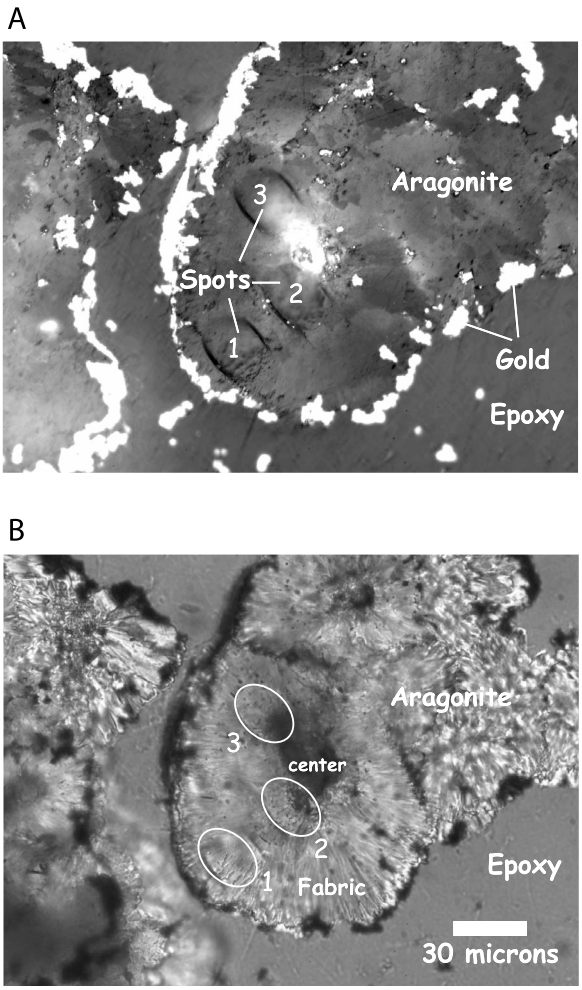

Figure 2. (a) Reflected and (b) transmitted light images of polished aragonite spherulites after SIMS analyses. The exposed surface of aragonite hemispheres is reasonably expected to have been attached to the growth substrate (beaker walls or stir rod), and therefore, the center of nucleation of any particular spherulite would be in its center. Patchy residual Au coating from SIMS analysis is visible in Figures 2a and 2b. SIMS ion beam craters are visible in Figure 2a and are marked by white ovals in Figure 2b. The numbers of the analysis spots are identical in both images. Spot 1 was collected on the spherulite fibers (rim), whereas spots 2 and 3 cover both the fibers and center areas.

Table 1. Reference $^{7}Li/^{6}Li$ Data[a]

Sample	$^{7}Li/^{6}Li$, Aragonite ICP-MS[b]	$\delta^{7}Li$, Aragonite ICP-MS	$^{7}Li/^{6}Li$, Fluid ICP-MS	$\delta^{7}Li$, Fluid ICP-MS	$\alpha(^{7}Li/^{6}Li)$ Aragonite-Fluid ICP-MS	$^{7}Li/^{6}Li$, Aragonite SIMS	$\delta^{7}Li$, Aragonite SIMS	Rate (μmol/min)
PGLi-4	12.835 (6)	67.8 (5)	12.970 (3)	79.1 (2)	0.9895 (7)	12.819 (12)	66.6 (1.0)	0.25
PGLi-6	12.8515 (7)	69.25 (6)	12.9679 (15)	78.92 (13)	0.9910 (1)	12.851 (8)	69.2 (7)	15.9
PGLi-5	12.8640 (9)	70.28 (8)	12.9634 (7)	78.56 (6)	0.9923 (2)	na		6.2

[a]Prior to normalizing to LSVEC SIMS data were corrected to PGLi-6 that was used as internal standard. Average aragonite precipitation rate was assumed to be proportional to the pumping rate of 0.023M Na_2CO_3. Units in parentheses represent 1 standard error (1 SE) in terms of least units cited, on the basis of replicate MC-ICP-MS and multispot SIMS analyses. Therefore, 12.835 (6) should be read as 12.835 ± 0.006. Uncertainties for SIMS data are 1 SE of the averages of 20 and 21 spots analyses in PGLi-4 and PGLi-6, respectively. MC-ICP-MS analyses of the main Li source (Li_2CO_3) yielded $\delta^{7}Li$ of 81.3 ± 0.3‰.

[b]Multicollector ICP-MS. MC-ICP-MS and SIMS data were normalized to LSVEC standard, where $^{7}Li/^{6}Li = 12.0192$ and $\delta^{7}Li = 0$‰ [*Flesch et al.*, 1973].

to be evaluated in order to improve our understanding of their relationships to temperature.

[5] Previous work has established the usefulness of in situ analyses of natural and experimental calcium carbonates using SIMS in combination with bulk analysis of carbonates and fluids by ICP-MS [e.g., *Sano et al.*, 2005; *Shirai et al.*, 2005; *Gabitov et al.*, 2006, 2008; *Gaetani and Cohen*, 2006; *Vigier et al.*, 2007; *Shirai et al.*, 2008; *Rollion-Bard et al.*, 2009; *Kasemann et al.*, 2009]. Here, we use SIMS to quantify $\delta^{7}Li$ and Li/Ca using internal (e.g., our aragonite) and external standardization on materials that compositionally match those of our samples (e.g., calcite CAL-HTP [*Vigier et al.*, 2007; *Rollion-Bard et al.*, 2009]). In order to determine Mg/Ca the calcite from Mexico described by *Kunioka et al.* [2006] and *Shirai et al.* [2008] was used. The goal of the present work is to determine $\delta^{7}Li$, Li/Ca, and Mg/Ca in morphologically different zones of aragonite, i.e., spherulite centers and fibers using SIMS and compare the obtained in situ data with the bulk ICP-MS analyses.

2. Experimental and Analytical Methods

2.1. Aragonite Precipitation

[6] Techniques employed for precipitating synthetic aragonites from seawater were adopted from *Kinsman and Holland* [1969] as modified by *Gabitov et al.* [2006]. Experiments have been conducted at Woods Hole Oceanographic Institution (WHOI). Seawater was collected from Vineyard Sound, Massachusetts. Crystallization of aragonite has been achieved by elevating seawater Ω by continuous addition of 0.023M aqueous Na_2CO_3 solution. To preclude the dilution of the growth medium, the doubly concentrated seawater (2SW) solution was introduced at the same time. For 2SW preparation, 1L of seawater was evaporated to half of its volume at 85°C in a PTFE beaker using an isothermal bath (Lauda RE-106). The amount of seawater that evaporated was calculated by the weight loss of the fluid. Addition of deionized H_2O adjusted the final mass of solution to half of initial producing the 50% evaporated seawater solution. ICP-MS analyses confirmed that concentrations of Mg, Ca, Sr, and Ba in 2SW solution were near double the values of those in seawater [*Gabitov et al.*, 2006]. Both solutions (Na_2CO_3 and 2SW) were injected simultaneously at the same rate by using a syringe pump. The injection rates were 0.011, 0.038, 0.27, 0.69, and 7.3 ml/min, which is equivalent to 0.25, 0.87, 6.2, 15.9, and 168 μmol of Na_2CO_3 per minute injection for the runs PGLi-4, PGLiB-1, PGLi-5, PGLi-6, and PGLi-2 respectively. In our study, these pumping rates are used as a proxy for relative precipitation rates of aragonite. *Gabitov et al.* [2006] and *Holcomb et al.* [2009] showed that aragonite growth rate positively correlates with the injection rate of Na_2CO_3 solution into seawater. 600 ml of seawater was continuously stirred at 120 rpm in the PTFE beaker using a PTFE propeller rod at 25°C. Prior to initiation of pumping, high-purity Li_2CO_3 powder was dissolved in the seawater and titrates. As a result, Li concentration in all fluids was elevated by a factor of ~23 relative to natural seawater.

2.2. MC-ICP-MS Sample Preparation and Bulk Analysis

[7] Analyses of final fluids and bulk precipitates from the runs PGLi-4, PGLi-5, and PGLi-6 were carried out by solution MC-ICP-MS after ion chromatographic Li matrix separation. Isotopic composition of Li_2CO_3 was determined by the same method. Prior to liquid ion chromatography, the carbonate run products were dissolved in 2M HNO_3. The growth solutions and the dissolved carbonates

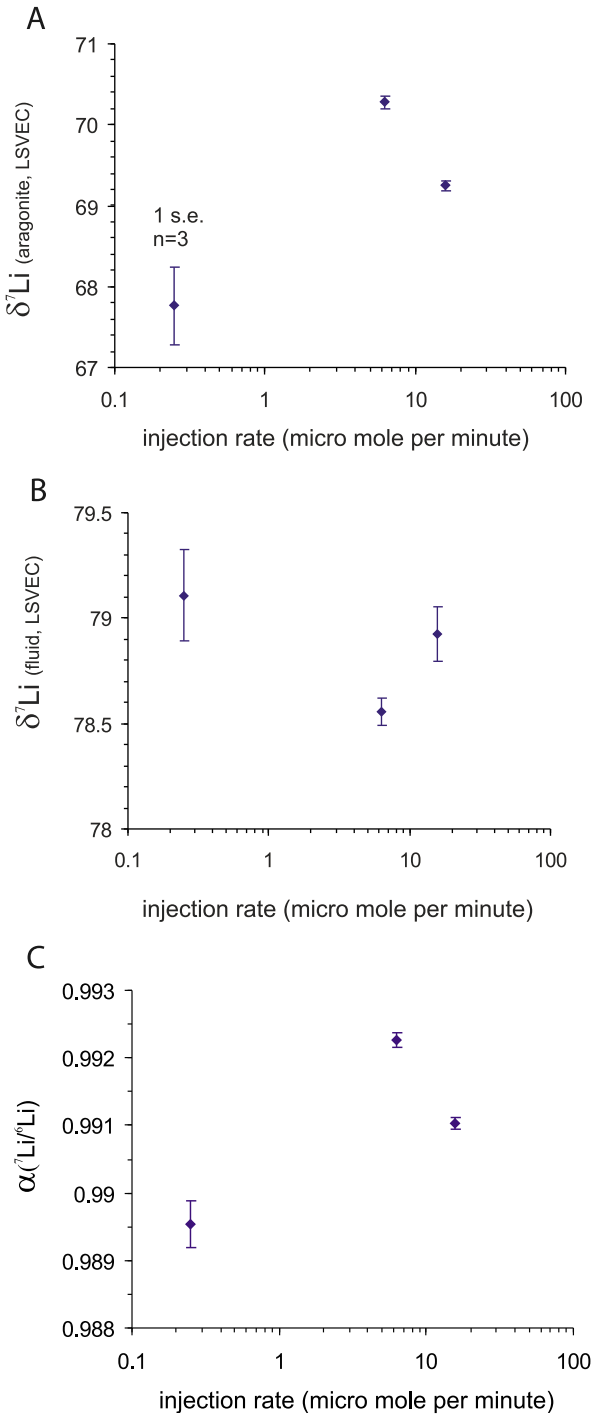

Figure 3. MC-ICP-MS results for three experiments plotted versus injection rate of 0.023M Na_2CO_3, which is proportional to aragonite precipitation rate. (a) δ^7Li of aragonites, (b) δ^7Li of fluids collected at the end of each run, and (c) fractionation factor (α) of ^{7}Li/^{6}Li between aragonite and fluid. Error bars are the standard errors (1 SE) from three replicate analyses of sample aliquots.

were evaporated to dryness and then dissolved in 9 ml 1N HNO_3 in 80% methanol (MeOH). Lithium matrix separation was carried out in glass columns filled with 10 ml cation resin Bio-Rad AG 50W X8 (200–400 mesh). Sample solutions (9 ml) were loaded on cleaned (40 ml 7N HNO_3) and conditioned (20 ml 0.1N HNO_3 in 50% MeOH) columns. After sample loading 10 ml of 1N HNO_3 in 80% MeOH were added before Li was finally eluted using 100 ml of 1N HNO_3 in 80% MeOH. Quantitative Li recovery and Li matrix separation were monitored by Li, Na, Sr, Nd and Pb concentration analyses of solutions collected prior to and after the Li elution. The determined Li procedural blanks of <0.5 ng for the used chemical method are negligible for the accuracy of the final δ^7Li values as >100 ng sample Li were run through chemistry.

[8] Lithium isotope ratio determinations were carried out on a MC-ICP-MS (NEPTUNE Thermo Fisher) at WHOI by sample standard bracketing after a method reported by *Rosner et al.* [2007]. The final separated samples were evaporated and then diluted in 0.5N HNO_3 to match the L-SVEC standard solutions (100, 50, 33, 10 μg g^{-1}) used for bracketing to within 5%. The Li isotope compositions are reported as ^{7}Li/^{6}Li normalized to L-SVEC [*Flesch et al.*, 1973] and were calculated by bracketing the measured ^{7}Li/^{6}Li of a sample with the mean of the two neighboring L-SVEC standards. Replicate measurements (n = 3) of our homogeneous sample solutions indicate δ^7Li reproducibility range of 0.1‰–0.5‰ (1 SE). Lithium isotope determination on multiple processed sample aliquots of IAPSO seawater and L-SVEC performed in the course of this study indicate an accuracy of the mean δ^7Li values of <0.5‰ and external reproducibility similar to that calculated here, i.e., <0.5‰ [*Rosner et al.*, 2007].

2.3. SIMS Sample Preparation and in Situ Analysis

[9] The beaker walls and the stir rod were rinsed with distilled water and methanol, and dried at 30°C. Spherulites grew outward from the rod and beaker walls, so the flat side of the aragonite hemispheres attached to the substrate. Spherulites were manually removed from the beaker and the rod using a spatula, and mounted in epoxy, such that the flat sides of the hemispheres were exposed for SIMS analysis. The mounts were polished with 1200 grit SiC paper followed by alumina powder (down to 1 μm size) and the spherulites were analyzed by using a CAMECA IMS 1270 ion microprobe with a 1.8–7.7 nA $^{16}O^-$

Table 2. SIMS Analyses of Reference Materials[a]

	^{7}Li	^{6}Li	^{7}Li/^{6}Li (1 SE) Raw	δ^{7}Li[b] (1 SE) ‰	^{24}Mg	^{42}Ca	^{24}Mg/^{42}Ca (1 SE) × 10^{2}	^{7}Li/^{42}Ca (1 SE) × 10^{2}
NIST-612 (δ^{7} = 31.2 ± 0.1‰[c]), 31 August 2009 (Session 1.4), FCp = 4.55 nA, 60 Cycles								
	288305	22663	12.721 (7)	31.9 (9)				
	295231	23214	12.718 (6)	31.7 (9)				
	301865	23738	12.716 (7)	31.5 (9)				
	278644	21943	12.698 (6)	30.1 (9)				
	298995	23528	12.708 (6)	30.9 (9)				
Mean			12.712	31.2				
1 SD			0.009	0.7				
NIST-612 (δ^{7} = 31.2 ± 0.1‰[c]), 23 November 2009 (Session 2.2), FCp = 2.5 nA, 30 Cycles								
	99503	7866	12.650 (11)	30.1 (1.5)	22632	274540	8.26 (5)	36.21 (11)
	99650	7860	12.678 (9)	32.3 (1.5)	22333	274247	8.16 (5)	36.33 (7)
	99755	7883	12.656 (10)	30.5 (1.5)	22283	273052	8.18 (6)	36.53 (6)
	98144	7757	12.653 (11)	30.3 (1.5)	21966	268503	8.19 (5)	36.55 (5)
	98228	7745	12.684 (9)	32.8 (1.5)	21896	267139	8.21 (6)	36.78 (6)
Mean			12.664	31.2			8.20	36.41
1 SD			0.016	1.3			0.04	0.219
NIST-614 (δ^{7} = 20.5 ± 0.1‰[c]), 31 August 2009 (Session 1.4), FCp = 4.47 nA, 60 Cycles								
	12722	1012	12.567 (18)	19.5 (1.6)				
	12667	1008	12.57 (2)	19.3 (1.9)				
	12347	982	12.577 (19)	20.2 (1.7)				
	12169	968	12.568 (19)	19.5 (1.7)				
	12486	992	12.59 (2)	21.3 (1.8)				
Mean			12.57	20.0				
1 SD			0.01	0.8				
NIST-610 (δ^{7} = 32.50 ± 0.02‰[c]), 23 November 2009 (Session 2.2), FCp = 2.3 nA, 30 Cycles								
	1114268	87899	12.678 (9)	32.3 (1.5)	163595	253565	64.6 (3)	439.7 (1.2)
	1118937	88066	12.706 (7)	34.6 (1.5)	165935	254571	65.2 (5)	439.9 (1.9)
	1125400	88588	12.705 (7)	34.5 (1.4)	167332	258466	64.8 (4)	435.8 (1.8)
Mean			12.696	33.8			64.9	439.8
1 SD			0.016	1.3			0.3	2.3
CAL-HTP, 23 November 2009 (Session 2.2), FCp = 1.8 nA, 60 Cycles								
	3359	274	12.23 (5)			296912		1.131 (5)
	3329	272	12.23 (3)			290735		1.145 (4)
	3582	294	12.16 (3)			287614		1.244 (6)
	3254	267	12.20 (3)			283787		1.146 (4)
	3177	260	12.20 (3)			277531		1.145 (3)
	3078	253	12.17 (3)			267194		1.152 (4)
	3210	262	12.27 (5)			266615		1.202 (8)
	3157	258	12.23 (5)			257292		1.226 (7)
Mean			12.21					1.174
1 SD			0.03					0.043
Calcite from Mexico, 23 November 2009 (Session 2.2), FCp = 1.8 nA, 30 Cycles[d]								
					75506	287905	26.2288 (497)	

[a]NIST-610, 612,614 = silicate glass; CAL-HTP = hydrothermally grown calcite [*Vigier et al.*, 2007]. ^{7}Li/^{6}Li are SIMS intensity ratios. Units in parentheses represent 1 standard error (1 SE = 1 SD/√n) in terms of least units cited, on the basis of replicate analyses.

[b]δ^{7}Li(LSVEC) for glasses were determined by correction to the internal standard NIST-612; therefore, the average δ^{7}Li in NIST-612 are the same as δ^{7}Li from *Kasemann et al.* [2005].

[c]MC-ICP-MS data from *Kasemann et al.* [2005].

[d]Reproducibility of calcite from Mexico was determined as 0.78% (1 SE, n = 6) in another SIMS session (not reported in this work). *Kunioka et al.* [2006] reported 1 SE = 1.29% for this material using NanoSIMS.

Table 3. IMF of $^{7}Li/^{6}Li$ and RIY of Li/Ca and Mg/Ca in the Reference Materials[a]

Material	Date	n	$^{7}Li/^{6}Li$ IMF (‰)	Li/Ca RIY	Mg/Ca RIY
Calcite (CAL-HTP)	23 Nov 2009	8	3.1 ± 1.0	2.85	
NIST-614 glass	31 Aug 2009	5	25.1 ± 0.4	na	na
NIST-612 glass	31 Aug 2009	5	25.7 ± 0.3	na	na
	20 Nov 2009	5	21.8 ± 0.6	0.91	0.45
NIST-610 glass	20 Nov 2009	3	23.1 ± 0.7	0.90	0.57
Average glass			23.9 ± 0.9	0.90	0.51

[a]RIY, relative ion yield of Li/Ca and Mg/Ca during SIMS measurements. Errors are 1 SE of multiple measurements in each subsession. Reference values of $^{7}Li/^{6}Li$ in glasses are 12.2656 (δ^{7} = 32.5‰), 12.3942 (δ^{7} = 31.2‰), and 12.4099 (δ^{7} = 20.5‰) in NIST-610, 612, and 614, respectively [*Kasemann et al.*, 2005]. Reference values of $^{7}Li/^{6}Li$ and Li/Ca in CAL-HTP are 12.1754 (δ^{7} = 13‰) and 28.9 μmol/mol (Li = 2ppm), respectively [*Rollion-Bard et al.*, 2009]. Reference value of Mg/Ca in Mexican calcite is 6.3 mmol/mol [*Kunioka et al.*, 2006]. Reference values of Li/Ca and Mg/Ca in NIST-610, 612, and 614 glasses are 3.42×10^{-2} and 9.38×10^{-3}, 2.81×10^{-3} and 1.50×10^{-3}, and 1.12×10^{-4} and 6.90×10^{-4} mol/mol, respectively [*Pearce et al.*, 1997; *Kasemann et al.*, 2005; *Shaheen et al.*, 2008].

primary beam at 20–30 μm lateral dimension on the sample surface. Positive secondary ions corresponding to mass/charge stations of 5.5 (background), ^{6}Li, and ^{7}Li were measured during analytical session 1 (August 2009). Subsequently, ^{24}Mg and ^{42}Ca were added to the previous set up in analytical session 2 (November 2009). Analytical sessions 1 and 2 consist of four and two subsessions, respectively, each subsession representing the interval of continuous operation of the duoplasmatron ion source (i.e., a ~12 h working period). Alignment of primary and secondary columns remained largely unchanged during each session. Intensities were measured by peak switching with waiting times up to 4 s and counting times of 1, 10, 4, 2, and 2 s for 5.5, ^{6}Li, ^{7}Li, ^{24}Mg, and ^{42}Ca, respectively. Each spot was presputtered until $^{7}Li/^{6}Li$ reached a steady state value. A mass resolving power (MRP) of ~2900 achieved separation of molecular interferences such as $^{23}Na^{1}H$, $^{26}Mg^{16}O$, $^{40}Ca^{1}H_{2}$ (Figure 1). $^{6}Li^{1}H$ was not detected at the relevant mass offset (0.0069 amu) from the ^{7}Li peak.

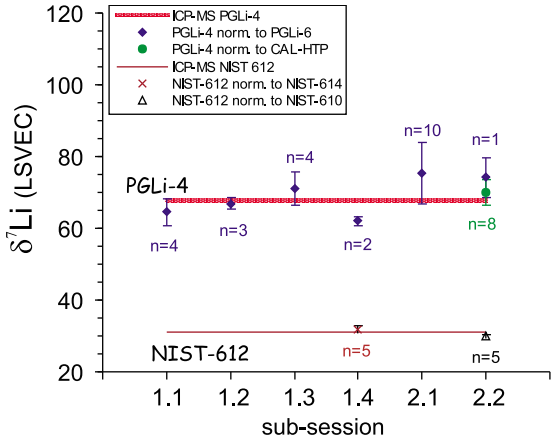

Figure 4. Li isotopic variability of NIST-612 and PGLi-4 during SIMS analytical sessions. Red horizontal bar represents the $\delta^{7}Li$ determined by MC-ICP-MS, with a thickness corresponding to $\delta^{7}Li \pm 1$ SD (this study). Diamonds are $\delta^{7}Li$ of PGLi-4 normalized to PGLi-6. Circle represents $\delta^{7}Li$ of aragonite 1 normalized to CAL-HTP. Brown horizontal line represents the $\delta^{7}Li$ determined by MC-ICP-MS [*Kasemann et al.*, 2005]. Cross and triangle are $\delta^{7}Li$ of NIST-612 normalized to NIST-614 and NIST-610, respectively. Each symbol represents the mean of $\delta^{7}Li$ determined in *n* number of spots; error bars are propagated from the 1 SD of the mean in the sample and reference material, except PGLi-4 data in subsession 2.2, where n = 1.

[10] An example of the polished aragonite spherulites is shown in Figure 2 in the reflected (Figure 2a) and transmitted light (Figure 2b) images. SIMS spot 1 was collected close to the rim of the spherulite and represents data from aragonite fibers only. Spots 2 and 3 were collected at areas that include both spherulite center and fibers.

[11] Reproducibility of $^{7}Li/^{6}Li$ in glasses (NIST-610, 612, 614) and calcite reference material (CAL-HTP) was 0.72‰–1.25‰ and 2.94‰ (1 SD), respectively. $^{7}Li/^{42}Ca$ and $^{24}Mg/^{42}Ca$ homogeneity in silicate glasses was <0.6%. CAL-HTP yielded $^{7}Li/^{42}Ca$ reproducibility of 3.7%. $\delta^{7}Li$ and Li in CAL-HTP were reported as 13‰ and 2 ppm, respectively

Table 4. IMF of $^{7}Li/^{6}Li$ in Aragonites[a]

Sample	Date	n	IMF (‰)
PGLi-4	27 Aug 2009	3	2.8 ± 1.7
	28 Aug2009	3	4.5 ± 0.9
	30 Aug 2009	4	8.1 ± 1.1
	31 Aug 2009	2	2.7 ± 0.4
	20 Nov 2009	10	6.3 ± 2.3
	23 Nov 2009	1	5.3
PGLi-6	27 Aug 2009	4	5.9 ± 0.9
	28 Aug 2009	2	5.3 ± 0.006
	30 Aug 2009	5	5.0 ± 1.6
	31 Aug 2009	2	8.1 ± 0.8
Average aragonite			5.4 ± 0.6

[a]IMF, instrumental mass fractionation of $^{7}Li/^{6}Li$; n, number of SIMS spots. Errors are 1 SE of multiple measurements in each subsession. Reference $^{7}Li/^{6}Li$ values are in Table 1.

Table 5. SIMS Analyses of Aragonites[a]

	^{7}Li	^{6}Li	$^{7}Li/^{6}Li$ (1 SE) Raw	$\delta^{7}Li$ (1 SE) ‰	^{24}Mg	^{42}Ca	$^{24}Mg/^{42}Ca$ (1 SE)	$^{7}Li/^{42}Ca$ (1 SE) × 10^{2}	Mg/Ca (mmol/mol)	Li/Ca (μmol/mol)
				PGLi-4, 27 August 2009 (Session 1.1), FCp = 3.6nA, 60 Cycles						
	35848	2798	12.813 (17)	60 (2)						
	31744	2463	12.890 (17)	66 (2)						
	29045	2252	12.90 (2)	67 (3)						
	32348	2511	12.881 (18)	65 (2)						
Mean			12.870	65						
1 SD			0.045	3						
				PGLi-4, 28 August 2009 (Session 1.2), FCp = 7.7nA, 60 Cycles						
	46777	3639	12.852 (15)	63.7 (1.6)						
	74731	5800	12.884 (15)	66.3 (1.5)						
	51158	3970	12.885 (14)	66.4 (1.5)						
Mean			12.874	65.5						
1 SD			0.019	1.5						
				PGLi-4, 30 August 2009 (Session 1.3), FCp = 5.0nA, 60 Cycles						
	49155	3806	12.915 (10)	69 (4)						
	66273	5126	12.928 (11)	70 (4)						
	32507	2514	12.93 (2)	70 (4)						
Mean			12.92	70						
1 SD			0.01	4						
				PGLi-4, 31 August 2009 (Session 1.4), FCp = 4.5nA, 60 Cycles						
	35352	2748	12.864 (14)	61.7 (1.7)						
	44426	3451	12.90 (10)	62.3 (1.5)						
Mean			12.87	62.0						
1 SD			0.05	1.6						
				PGLi-4, 20 November 2009 (Session 2.1), FCp = 2.1nA, 30 and 60 Cycles[b]						
f	6071	468	12.97 (5)	79 (5)	18611	223764	0.0832 (3)	2.715 (15)	1.998 (5)	67.4 (1.9)
c	12464	956	13.037 (19)	85 (3)	113887	281669	0.4044 (11)	4.424 (15)	9.71 (3)	110 (3)
f+c	12047	924	13.043 (19)	86 (3)	201096	279785	0.716 (6)	4.305 (9)	17.19 (6)	107 (3)
f	8604	664	12.96 (2)	79 (4)	29499	297800	0.0991 (1)	2.889 (6)	2.379 (6)	71.7 (1.9)
f + c	12414	970	12.79 (3)	65 (4)	42842	300017	0.1428 (2)	4.136 (9)	3.430 (9)	103 (3)
c	16891	1316	12.83 (2)	68 (4)	71649	314298	0.2280 (4)	5.370 (19)	5.477 (14)	133 (4)
f	9173	716	12.80 (3)	66 (4)	28742	298013	0.0964 (1)	3.077 (7)	2.316 (6)	76 (2)
f	11862	924	12.84 (3)	69 (4)	38374	307922	0.1247 (3)	3.851 (7)	2.995 (8)	96 (3)
c	22922	1767	12.97 (2)	79 (3)	340609	291120	1.170 (5)	7.86 (4)	28.09 (8)	195 (5)
f+c	12547	972	12.90 (3)	74 (4)	80385	277334	0.289 (3)	4.52 (3)	6.94 (3)	112 (3)
Mean			12.91	75			0.3	4.31	8.05	107
1 SD			0.09	8			0.3[c]	1.49	8.46[c]	37
Mean (f)			12.89	73			0.101	3.13	2.42	78
1 SD			0.08	6			0.017	0.50	0.42	12
				PGLi-4, 23 November 2009 (Session 2.2), FCp = 2.1nA, 30 Cycles[b]						
c	27748	2150	12.902 (19)	74.11 (13)	413050	270696	1.522 (9)	10.23 (8)	36.55 (11)	254 (7)
				PGLi-6, 27 August 2009 (Session 1.1), FCp = 3.9nA, 60 Cycles						
	47410	3668	12.926 (12)	69 (2)						
	43308	3358	12.894 (17)	67 (2)						
	54726	4228	12.942 (13)	70 (2)						
	34856	2692	12.95 (2)	71 (3)						
Mean			12.93	69						
1 SD			0.02	2						
				PGLi-6, 28 August 2009 (Session 1.2), FCp = 4.6nA, 60 Cycles						
	42695	3305	12.919 (12)	69.2 (1.4)						
	61015	4723	12.919 (10)	69.3 (1.3)						
Mean			12.919	69.2						
1 SD			0.011	1.3						

Table 5. (continued)

	^{7}Li	^{6}Li	^{7}Li/^{6}Li (1 SE) Raw	δ^{7}Li (1 SE) ‰	^{24}Mg	^{42}Ca	^{24}Mg/^{42}Ca (1 SE)	^{7}Li/^{42}Ca (1 SE) × 10^{2}	Mg/Ca (mmol/mol)	Li/Ca (μmol/mol)
				PGLi-6, 30 August 2009 (Session 1.3), FCp = 5.7nA, 60 Cycles						
	58520	4531	12.914 (12)	69 (4)						
	58081	4486	12.948 (11)	72 (4)						
	58880	4553	12.931 (9)	70 (4)						
	54110	4179	12.949 (11)	72 (4)						
	51299	3996	12.837 (17)	62 (4)						
Mean			12.916	69						
1 SD			0.046	4						
				PGLi-6, 31 August 2009 (Session 1.4), FCp = 4.5nA, 60 Cycles						
	76570	5913	12.948 (9)	68.6 (1.5)						
	74111	5717	12.963 (9)	69.9 (1.5)						
Mean			12.956	69.2						
1 SD			0.009	1.5						
				PGLi-6, 20 November 2009 (Session 2.1), FCp = 1.9nA, 30 Cycles[b,d]						
c	21017	1636	12.85 (3)	65 (4)	341168	263791	1.293 (2)	7.96 (3)	31.06 (8)	198 (5)
f	14320	1121	12.77 (3)	58 (4)	67428	275939	0.2445 (3)	5.186 (13)	5.872 (15)	129 (3)
c	22737	1767	12.86 (2)	66 (4)	329708	303184	1.083 (10)	7.49 (3)	26.00 (10)	186 (5)
f	13855	1082	12.80 (3)	61 (4)	74882	271845	0.2754 (3)	5.093 (15)	6.616 (17)	127 (3)
f+c	15597	1215	12.83 (3)	63 (4)	68384	297418	0.2300 (4)	5.240 (13)	5.526 (14)	130 (3)
f	11473	894	12.84 (3)	64 (4)	43653	275463	0.1584 (4)	4.161 (19)	3.806 (10)	103 (3)
c	13537	1051	12.877 (19)	67 (3)	301096	237949	1.262 (11)	5.67 (6)	30.31 (11)	141 (5)
f	9859	763	12.92 (3)	70 (4)	55415	249867	0.2218 (3)	3.941 (17)	5.328 (13)	98 (3)
Mean			12.84	64			0.596	5.593	14.31	139
1 SD			0.05	4			0.515	1.442	12.37	36
Mean (f)			12.83	63			0.225	4.595	5.41	114
1 SD			0.06	5			0.495	0.636	1.19	16
				PGLi-6, 23 November 2009 (Session 2.2), FCp = 1.7nA, 30 Cycles[b]						
	12166	944	12.88 (3)	68 (4)	51545	243205	0.2120 (5)	5.00 (2)	5.093 (13)	124 (3)
	17287	1349	12.81 (2)	63 (4)	165925	269081	0.6170 (19)	6.42 (2)	14.82 (4)	159 (4)
Mean			12.84	62			0.4145	5.71	9.96	142
1 SD			0.05	4			0.2863	1.01	6.88	25
				PGLiB-1, 27 August 2009 (Session 1.1), FCp = 3.6nA, 60 Cycles						
	33462	2592	12.910 (14)	68 (2)						
	34512	2672	12.91 (2)	68 (3)						
Mean			12.912	68						
1 SD			0.014	2						
				PGLiB-1, 28 August 2009 (Session 1.2), FCp = 4.6nA, 60 Cycles						
	87038	6750	12.895 (13)	67.2 (1.4)						
	85560	6636	12.894 (10)	67.1 (1.2)						
Mean			12.894	67.2						
1 SD			0.011	0.1						
				PGLiB-1, 31 August 2009 (Session 1.4), FCp = 4.5 nA, 60 Cycles						
	76570	5913	12.948 (9)	68.6 (1.5)						
	74111	5717	12.963 (9)	69.9 (1.5)						
Mean			12.956	69.2						
1 SD			0.009	1.5						
				PGLiB-1, 20 November 2009 (Session 2.1), FCp = 2 nA, 30 Cycles						
	709	9176	12.94 (2)	77 (4)	92869	279655	0.3321 (13)	3.280 (12)	7.976 (10)	81 (2)
	586	7656	13.06 (2)	87 (4)	95377	242321	0.3935 (6)	3.156 (12)	9.452 (5)	78 (2)
	219	2838	12.98 (4)	80(5)	38473	126414	0.3038 (12)	2.23 (2)	7.298 (9)	55.5 (1.8)
Mean			12.99	82			0.3431	2.89	8.242	72
1 SD			0.06	5			0.0459	0.57	1.102	14

Table 5. (continued)

^{7}Li	^{6}Li	^{7}Li/^{6}Li (1 SE) Raw	δ^{7}Li (1 SE) ‰	^{24}Mg	^{42}Ca	^{24}Mg/^{42}Ca (1 SE)	^{7}Li/^{42}Ca (1 SE) × 10^{2}	Mg/Ca (mmol/mol)	Li/Ca (μmol/mol)
PGLiB-1, 23 November 2009 (Session 2.2), FCp = 1.5 nA, 30 Cycles[b]									
12551	980	12.81 (3)	66 (4)	110659	296376	0.3737 (13)	4.233 (14)	8.975 (10)	105 (2)
PGLi-2, 27 August 2009 (Session 1.1), FCp = 3.6 nA, 60 Cycles									
34164	2645	12.916 (17)	68 (2)						
PGLi-2, 28 August 2009 (Session 1.2), FCp = 11.7 nA, 60 Cycles									
77486	6019	12.873 (10)	65.4 (1.2)						
34164	2645	12.977 (15)	74.0 (1.5)						
PGLi-2, 20 November 2009 (Session 2.1), FCp = 2 nA, 30 Cycles									
13894	1081	12.84 (3)	69 (5)	211323	306031	0.690 (3)	4.53 (3)	16.57 (5)	112 (3)

[a] ^{7}Li/^{6}Li are SIMS intensity ratios. δ^{7}Li was determined by normalizing to SIMS and MC-ICP-MS data of PGLi-6 (except session in November 2009). c, f, and f+c are spherulite centers, fiber aragonite, and their mixture, respectively; mean (f) is the average of fiber data. 1 SD is the external standard deviation or the mean of the internal 1 SE; the largest one is presented. Please note that during session 1 δ^{7}Li values of aragonite samples were calculated using SIMS and ICP-MS data of PGLi-6, which is less heterogeneous than PGLi-4 but not homogeneous enough to be treated as a standard. Therefore, 1 SE of δ^{7}Li are significantly larger (by a factor of ~1.5) than 1 SE of raw SIMS ^{7}Li/^{6}Li data.

[b] δ^{7}Li was determined by normalizing to our SIMS data and bulk data reported by *Rollion-Bard et al.* [2009] for CAL-HTP; these δ^{7}Li data overlap with those determined by normalizing to PGLi-6 within 1 SE.

[c] Statistically insignificant value because high heterogeneity of the sample.

[d] Li/Ca and Mg/Ca in subsession 2.1 were estimated from the next subsession (2.2) analyses of CAL-HTP.

[*Rollion-Bard et al.*, 2009]. The Li/Ca was estimated as 28.9 μmol/mol by assuming stoichiometric Ca content in calcite of 4×10^{5} ppm (presence of Li has negligible effect on these calculations relative to SIMS analytical uncertainties). Reference value of Mg/Ca in Mexican calcite is 6.3 mmol/mol [*Kunioka et al.*, 2006; *Shirai et al.*, 2008].

3. Results

3.1. MC-ICP-MS Data

[12] The mean of three replicates of the bulk MC-ICP-MS analysis of three aragonite samples yielded that δ^{7}Li increases by 2.5‰ when Na_2CO_3 injection rate increases from 0.25 to 6.2 μmol/min, then δ^{7}Li decreases by 1‰ at the fastest injection rate of 15.9 μmol/min (Table 1 and Figure 3a). δ^{7}Li in PGLI-4 and PGLi-6 fluids is homogeneous within 1 SE uncertainty (Figure 3b). However, fluid δ^{7}Li is 0.5‰ lower in PGLi-5. We calculate an isotopic fractionation factor using the bulk ^{7}Li/^{6}Li of experimental aragonite and the final fluid

$$\left(\alpha = \frac{\left(^{7}Li/^{6}Li\right)_{solid}}{\left(^{7}Li/^{6}Li\right)_{fluid}}\right) \quad (1)$$

The plot of α values versus precipitation rate shows the similar pattern as for aragonite δ^{7}Li (Figure 3c). Here α varies between 0.9895 ± 0.0007 and 0.9923 ± 0.0002, i.e., from −10.5‰ to −7.7‰. This range overlaps with aragonitic corals (~−9‰ [*Marriott et al.*, 2004a]), but extend the range observed in synthetic aragonites (~−12‰ [*Marriott et al.*, 2004b]) and alteration aragonite veins in altered oceanic crust (−16‰ to −10‰ [*Rosner et al.*, 2004]).

[13] Li isotopic composition of the initial fluid (solution at the beginning of the experiments) was calculated using measured δ^{7}Li of the main Li source (Li_2CO_3, δ^{7}Li = +81.3 ± 0.3‰, molar fraction of

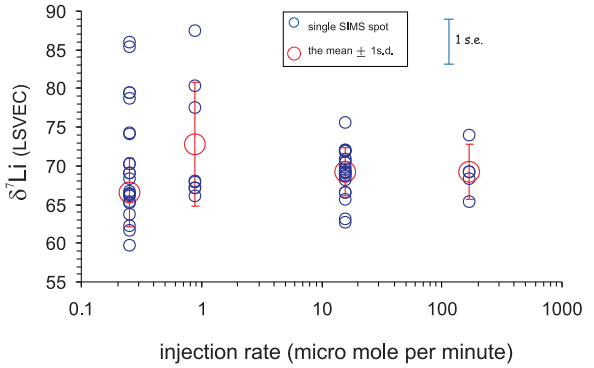

Figure 5. δ^{7}Li from four aragonite samples (PGLi-4, PGLiB-1, PGLi-6, and PGLi-2). Small circles represent individual spot analyses (see 1 SE example bar on the plot). Large circles are the averages of multiple SIMS data with 1 SD error bars.

22/23) and averaged seawater value (δ^7Li ≈ +33‰, molar fraction of 1/23). The following mass balance equation was used:

$$\delta^7Li(initial\ fluid) = 22/23 \times \delta^7Li(Na_2CO_3) + 1/23 \times \delta^7Li(seawater) = 79.2‰ \quad (2)$$

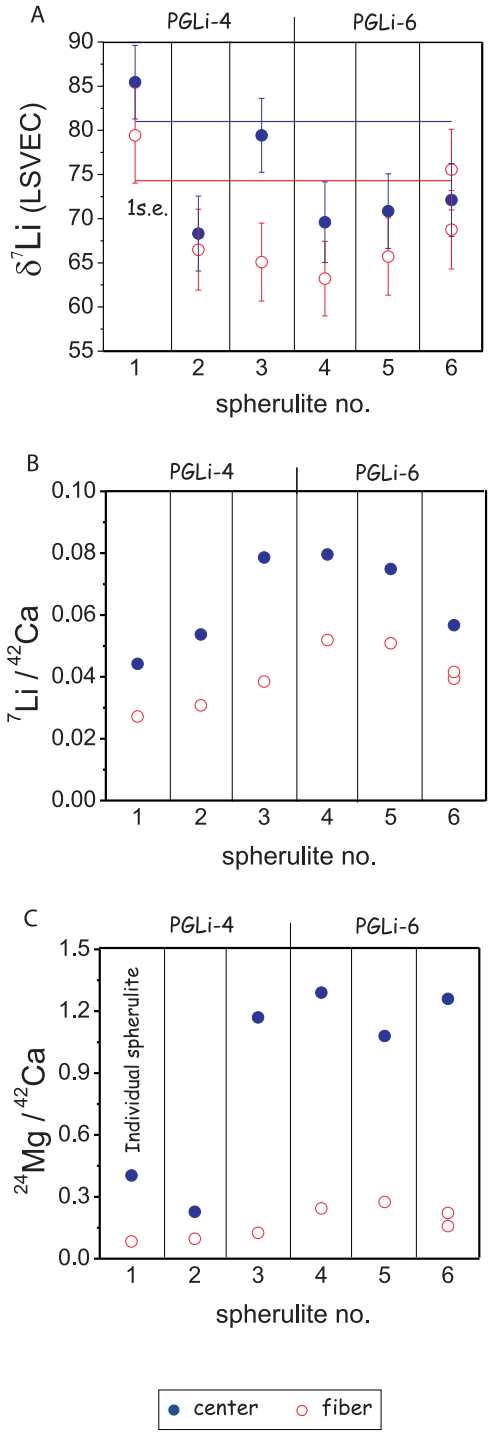

This initial fluid δ^7Li is similar to the measured δ^7Li in the final solutions (Table 1). Therefore, fluid ^{7}Li/^{6}Li was assumed to be constant over the duration of the runs.

3.2. SIMS Data

[14] Isotopically homogeneous silicate glass standards (NIST-610, 612, and 614) were examined in order to test instrumental reproducibility (Table 2). *Kasemann et al.* [2005] reported MC-ICP-MS and in situ SIMS δ^7Li data that showed that these standard glasses are enriched in ^{7}Li and homogeneous within 1 SD of 0.01‰–0.07‰ (two measurements of one aliquot) in MC-ICP-MS, and 1 SD of 0.9‰–2.8‰ (ten spots) in SIMS, measurements. Our SIMS δ^7Li five spot analyses of NIST-612 and 614 glasses yielded reproducibility within 1 SD 0.8‰–1.3‰ (1 SD of ^{7}Li/^{6}Li intensity ratios varied from 0.7‰ to 1.2‰). Internal (single spot) standard error (1 SE) of 0.5‰–0.8‰ was determined through the averaging of ^{7}Li/^{6}Li intensity ratios in 30 or 60 analytical cycles. The isotopic discrimination in SIMS is characterized by an instrumental mass fractionation factor (IMF):

$$IMF = \left(\frac{\left(^7Li/^6Li\right)^{SIMS}}{\left(^7Li/^6Li\right)^{reference}} - 1 \right) \cdot 10^3‰ \quad (3)$$

Using values from *Kasemann et al.* [2005], we found that the IMF for silicate glasses varied between 25.7 ± 0.3‰ (1 SE) (MSWD = 1.2, n = 5) and 21.8 ± 0.6‰ (MSWD = 1.2, n = 5) throughout the analytical sessions with an average of 23.9 ± 0.9‰ (Table 3). We determined IMF on NIST-614 and 610 and applied these values to NIST-612 in order to check for internal consistency between bulk MC-ICP-MS and multiple SIMS spot analyses (Table 2 and Figure 4). Each symbol represents

Figure 6. Comparison of SIMS (a) δ^7Li, (b) ^{7}Li/^{42}Ca, and (c) ^{24}Mg/^{42}Ca collected in spherulite centers (solid symbols) and fibers (open symbols) of experimentally precipitated abiogenic aragonite spherulites. Each column includes the data from an individual spherulite. In Figure 6a, blue and red solid lines are the averages for δ^7Li in the aragonite centers and fibers, respectively. In Figures 6b and 6c, the error bars (1 SE) are smaller than the size of the markers on the plots of ^{7}Li/^{42}Ca and ^{24}Mg/^{42}Ca. The lateral dimensions of the O^- beam are larger than the spherulite centers, and therefore, solid symbols represent compositions for centers and fibers (for example, see spots 2 and 3 in Figure 2). All data are from session 2.1.

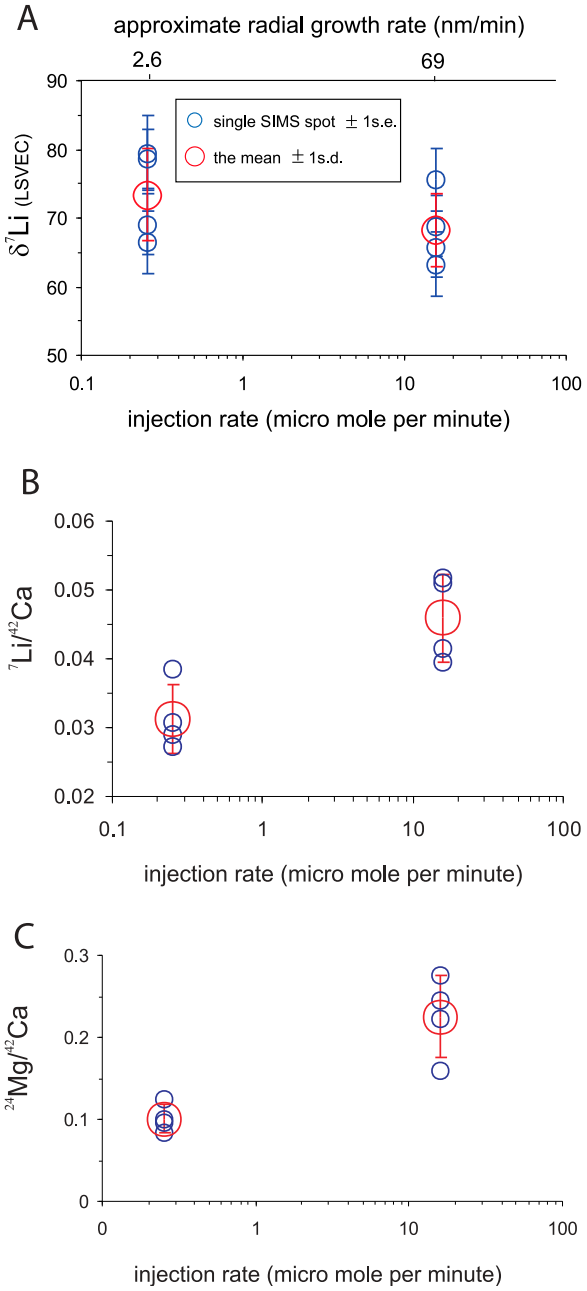

Figure 7. Variation of SIMS (a) δ^7Li, (b) ^{7}Li/^{42}Ca, and (c) ^{24}Mg/^{42}Ca with aragonite precipitation rate. The bottom x axis shows the bulk precipitation rate expressed as the injection rate of the titrant (Na_2CO_3). The top x axis represents the radial spherulite growth rates determined in the same samples by *Gabitov et al.* [2006]. The data presented here were collected at the aragonite fibers. Each small blue circle corresponds to the single spot analysis with the error bar of internal 1 SE. The averages of these data are shown as large red circles with the error bar of external 1 SD between individual spot data for each of the two runs. All data are from session 2.1.

the average of replicates analyzed during individual subsessions (i.e., alternating between NIST-612, 614, and 610). In two subsessions δ^7Li SIMS data of NIST-612 are consistent with independently determined δ^7Li MC-ICP-MS value of this standard (brown line, from *Kasemann et al.* [2005]).

[15] Analyses of Li-doped calcite quality control material (CAL-HTP) yielded ^{7}Li/^{6}Li external reproducibility of 2.5‰ (1 SD) and IMF of 3.1 ± 1.0‰ (1 SE, n = 8) (Table 3). The mean IMF for aragonite in PGLi-4 and PGLi-6 was 5.4 ± 0.6‰ (Table 4) (all material of PGLi-5 was consumed by MC-ICP-MS analyses). The observed similar IMF for aragonite and calcite is expected to be a common phenomenon as the main chemical composition is comparable and only minor chemical and crystallographic differences exist between the two materials. This conclusion is supported by similarity of SIMS IMF of ^{11}B/^{10}B for basaltic to rhyolitic natural glasses [*Rosner et al.*, 2008].

[16] The variability of δ^7Li measured in aragonite ranges from 1 SD = 1.3‰ to 8‰ (^{7}Li/^{6}Li SIMS intensity ratios range from 1 SD = 0.6‰ to 7.1‰) in different subsessions. The reasons for that are the variability in number of SIMS measurements and Li count rates that are related to $^{16}O^-$ primary beam current. Therefore, to assess heterogeneity in the samples, it is important to compare the variation of the standards and samples in the same session only. The standard deviation for CAL-HTP and especially NIST glasses within a session are always lower than in aragonite samples from the same analytical session (Tables 2 and 5). Similarly to silicate glasses, ^{7}Li/^{6}Li of aragonite from PGLi-4 was normalized to aragonite from PGLi-6 (Figure 4). In five subsessions, δ^7Li SIMS data of the run PGLi-4 (diamonds) are consistent with independently determined δ^7Li MC-ICP-MS value of this sample (red bar). The only exception is δ^7Li of the run PGLi-4 obtained in subsession 1.4, where only two spots were measured, which resulted in a typically small error bars. In subsession 2.2, we also used the IMF value determined by analysis of CAL-HTP which yielded a value for PGLi-4 that is consistent with that obtained by using the IMF determined by analysis of sample PGLi-6 (circle).

[17] Relative ion yields of Li/Ca:

$$\left(RIY = \frac{\left(^7Li/^{42}Ca\right)^{SIMS}}{\left(^7Li/^{42}Ca\right)^{true}} \cdot \frac{abundance(\%^{42}Ca)}{abundance(\%^7Li)} \right) \quad (4)$$

were calculated from analysis of CAL-HTP assuming the natural abundances of ^{7}Li (92.5%) and ^{42}Ca (0.648%). Mg/Ca RIY was calculated similarly with a ^{24}Mg natural abundance of 79.0% and by using the elemental concentrations for optically clear calcite from Mexico (Table 3) [*Kunioka et al.*, 2006].

[18] Compositions of the spherulites ranged significantly in each sample. 1 SD was as high as 8‰, >30%, and >100% for ^{7}Li/^{6}Li, ^{7}Li/^{42}Ca, and ^{24}Mg/^{42}Ca, respectively (Table 5 and Figure 5 for δ^{7}Li). However, this large variability in ^{7}Li/^{42}Ca and ^{24}Mg/^{42}Ca was reduced by considering only analyses of fibrous aragonite. Li/Ca and Mg/Ca in the sessions 2.1 and 2.2 were estimated by using CAL-HTP quality control material that was measured during session 2.2. Because of the lack of CAL-HTP analyses in the session 2.1, Li and Mg data are presented as raw SIMS intensity ratios in Figures 6 and 7. Figure 6 shows δ^{7}Li, ^{7}Li/^{42}Ca, and ^{24}Mg/^{42}Ca data collected in spherulite centers and fibers of aragonites from PGLi-4 and PGLi-6 (three spherulites in each sample). δ^{7}Li differences between spherulite centers (closed circles) and fibers (open circles) are almost indistinguishable (Figure 6a). However, the mean δ^{7}Li of the data points collected at spherulite centers (blue line) is slightly higher than the mean of the data points collected at aragonite fibers (red line). This effect is much stronger for elemental ratios, Li/Ca and Mg/Ca are enriched in spherulite centers relative to aragonite fibers by factors of 2 and 8, respectively (Figures 6b and 6c).

4. Discussion

[19] Similar to the present work, SIMS analyses of deep sea corals yield overlapping of δ^{7}Li in COCs and fibers of the coral septa (Figure 6a) [*Rollion-Bard et al.*, 2009]. However, both works show a slightly lower δ^{7}Li in fibers relative to centers. Therefore, it is probably premature to eliminate the possibility of δ^{7}Li dependence on the type of mineralization zone of biogenic and abiogenic aragonites, although any precipitation rate dependence appears to be weak. The similarity in variation of δ^{7}Li in synthetic aragonite (this work) and corals [*Rollion-Bard et al.*, 2009] suggests that biological control on ^{7}Li/^{6}Li fractionation is insignificant. The growth rate effect on Li isotopic composition in aragonite was not resolved because the variability of δ^{7}Li data between multiple SIMS spots of the single sample (the range of up to 27‰) masked small differences in mean δ^{7}Li between aragonites precipitated at different rates (the range of up to 6‰) (Figures 5 and 7a).

[20] For elemental ratios, ^{7}Li/^{42}Ca and ^{24}Mg/^{42}Ca, in order to reduce scatter within a single sample, spherulite center data were excluded from data set and only fibers data were plotted versus precipitation rate in Figures 7b and 7c. Here all data were collected during single session 2.1. The bottom and top x axes represent the Na_2CO_3 injection rates and radial growth rates of spherulites determined in the same runs by *Gabitov et al.* [2006] using Sr isotope markers. The growth rates of the spherulites edge fibers determined in their study are 2.6 ± 1.3 and 69 ± 14 nm/min for aragonites in PGLi-4 and PGLi-6, respectively. Growth of spherulite edge fibers is slower than precipitation of spherulite centers [*Gabitov et al.*, 2008; *Holcomb et al.*, 2009]. Therefore, each of the two radial rate values presented above is lower than the mean growth rate of aragonite in corresponding run (PGLi-4 or PGLi-6). The δ^{7}Li heterogeneity of aragonite fibers from the single run means that the difference in δ^{7}Li between samples precipitated at different rates cannot be resolved unlike bulk MC-ICP-MS results where errors represent not the heterogeneity but the analytical uncertainty only (Figures 7a and 3a).

[21] The Mg/Ca enrichment in aragonite spherulite centers is consistent with results found previously by *Gabitov et al.* [2008] and *Holcomb et al.* [2009], where high Mg/Ca in the center was explained by its enhanced growth rate. The similarity of Li/Ca and Mg/Ca distribution in both abiogenic aragonites and corals suggest that $K_d^{Li/Ca}$ positively correlates with crystallization rate, as was shown for $K_d^{Mg/Ca}$ [*Gabitov et al.*, 2006, 2008]. In addition, positive correlations of ^{7}Li with ^{24}Mg SIMS intensities (linear regression slope of 0.04, $R^2 = 0.78$) qualitatively agrees with findings of *Case et al.* [2010] in corals suggesting the similarity of Li and Mg behavior during precipitation of synthetic and biogenic aragonite. Overall, the separation of Mg/Ca and Li/Ca of coral fibers from its COC's data should increase the precision of their temperature calibrations and ocean budget proxies.

[22] The heterogeneity observed in individual samples in ^{7}Li/^{42}Ca and ^{24}Mg/^{42}Ca means that dependence on aragonite precipitation rate can be resolved by SIMS when data collected in spherulite centers are separated from those in aragonite fibers. Excluding of the data from spherulite centers yields an increase of ^{7}Li/^{42}Ca and ^{24}Mg/^{42}Ca with increasing precipitation rate (Figures 7b and 7c). Here the

means of $^{7}Li/^{42}Ca$ and $^{24}Mg/^{42}Ca$ in the fast precipitated run (PGLi-6) are higher than in the slow run (PGLi-4) by ~50% and ~120%, respectively. Thus, both observations shown in Figures 6 and 7 suggest a positive correlation of Li/Ca with aragonite growth rate. This Li/Ca growth rate dependence is significant but somewhat weaker than that of Mg/Ca. *Gabitov et al.* [2008] explained Mg/Ca increase with aragonite crystallization rate using the growth entrapment model developed by Watson and coworkers [*Watson and Liang*, 1995; *Watson*, 1996, 2004]. It was proposed that enhanced crystal growth rates cause entrapment of crystal surface composition by the newly formed lattice. Results from our present work suggest that Li partitioning could also be explained by a growth entrapment model, however, more data are required to confirm this suggestion.

5. Summary

[23] We demonstrate that $\delta^{7}Li$ in experimentally precipitated aragonites determined by MC-ICP-MS and SIMS agrees when SIMS analyses are corrected for IMF using either calcite or experimental aragonite references. SIMS data does not yield a relationship between $^{7}Li/^{6}Li$ fractionation and aragonite precipitation rate at the range of Na_2CO_3 injection rate from 0.25 to 168 μmol/min. However, given the lack of growth rate information and the significant heterogeneity within single samples, it is premature to rule out any effect of growth kinetics on $^{7}Li/^{6}Li$ fractionation between aragonite and fluid. Li/Ca and Mg/Ca are sensitive to aragonite growth rate within a single spherulite. The dependence on bulk precipitation rate is resolvable only after exclusion of data from spherulite centers, which are systematically enriched in Li/Ca and Mg/Ca. This enrichment likely reflects faster precipitation of the spherulites centers relative to the fibrous aragonite. Therefore, taking into account the potential effects of coral growth rates can improve Li/Ca and Mg/Ca temperature calibrations, and the reliability of the Li isotope proxy for past seawater compositions.

Acknowledgments

[24] We thank Fabrice Brunet, Claire Rollion-Bard, and Kotaro Shirai for providing calcite standards for normalization of ion probe data. We also thank the Editor, Joel Baker, and two anonymous reviewers for their comments on the manuscript. SIMS analyses were supported by U.S. NSF, EAR, Instrumentation and Facilities Program. The development of the method for bulk $\delta^{7}Li$ analysis and the MC-ICP-MS measurements were covered by NSF grant EAR/IF-0318137. Precipitation experiments were supported by NSF through grants OCE-0402728, OCE-0527350, and OCE-0823527 to Glenn Gaetani and Anne Cohen and through grant EAR-0337481 to Bruce Watson.

References

Bryan, S. P., and T. M. Marchitto (2008), Mg/Ca-temperature proxy in benthic foraminifera: New calibrations from the Florida Straits and a hypothesis regarding Mg/Li, *Paleoceanography*, *23*, PA2220, doi:10.1029/2007PA001553.

Case, D. H., L. F. Robinson, M. E. Auro, and A. C. Gagnon (2010), Environmental and biological controls on Mg and Li in deep-sea scleractinian corals, *Earth Planet. Sci. Lett.*, *300*, 215–225, doi:10.1016/j.epsl.2010.09.029.

Chan, L.-H., J. M. Edmond, and G. Thompson (1993), A lithium isotope study of hot springs and metabasalts from mid-ocean ridge hydrothermal systems, *J. Geophys. Res.*, *98*, 9653–9659, doi:10.1029/92JB00840.

Chan, L.-H., J. M. Gieskes, C. F. You, and J. M. Edmond (1994), Lithium isotope geochemistry of sediments and hydrothermal fluids of the Guaymas Basin, Gulf of California, *Geochim. Cosmochim. Acta*, *58*, 4443–4454, doi:10.1016/0016-7037(94)90346-8.

Coplen, T. B., et al. (2002), Compilation of minimum and maximum isotope ratios of selected elements in naturally occurring terrestrial materials and reagents, *U.S. Geol. Surv. Water Resour. Invest. Rep., 01-4222*, 98 pp.

Delaney, M. L., A. W. H. Be, and E. A. Boyle (1985), Li, Sr, Mg, and Na in foraminiferal calcite shells from laboratory culture, sediment traps, and sediment cores, *Geochim. Cosmochim. Acta*, *49*, 1327–1341, doi:10.1016/0016-7037(85)90284-4.

Delaney, M. L., B. N. Popp, C. G. Lepzelter, and T. F. Anderson (1989), Lithium-to-calcium ratios in Modern, Cenozoic, and Paleozoic articulate brachiopod shells, *Paleoceanography*, *4*(6), 681–691, doi:10.1029/PA004i006p00681.

Flesch, G. D., A. R. Anderson, and H. J. Svec (1973), A secondary isotopic standard for $^{6}Li/^{7}Li$ determination, *Int. J. Mass Spectrom. Ion Phys.*, *12*, 265–272, doi:10.1016/0020-7381(73)80043-9.

Gabitov, R. I., A. L. Cohen, G. A. Gaetani, M. Holcomb, and E. B. Watson (2006), The impact of crystal growth rate on element ratios in aragonite: An experimental approach to understanding vital effects, *Geochim. Cosmochim. Acta*, *70*(18), suppl., A187, doi:10.1016/j.gca.2006.06.377.

Gabitov, R. I., G. A. Gaetani, E. B. Watson, A. L. Cohen, and H. L. Ehrlich (2008), Experimental determination of growth rate effect on U^{6+} and Mg^{2+} partitioning between aragonite and fluid at elevated U^{6+} concentration, *Geochim. Cosmochim. Acta*, *72*, 4058–4068, doi:10.1016/j.gca.2008.05.047.

Gaetani, G. A., and A. L. Cohen (2006), Element partitioning during precipitation of aragonite from seawater: A framework for understanding paleoproxies, *Geochim. Cosmochim. Acta*, *70*, 4617–4634, doi:10.1016/j.gca.2006.07.008.

Gagnon, A. C., J. F. Adkins, D. P. Fernandez, and L. F. Robinson (2007), Sr/Ca and Mg/Ca vital effects correlated with skeletal architecture in a scleractinian deep-sea coral and the role of

Rayleigh fractionation, *Earth Planet. Sci. Lett.*, *261*, 280–295, doi:10.1016/j.epsl.2007.07.013.

Hall, J. M., and L. H. Chan (2004), Li/Ca in multiple species of benthic and planktonic foraminifera: Thermocline, latitudinal, and glacial-interglacial variation, *Geochim. Cosmochim. Acta*, *68*, 529–545, doi:10.1016/S0016-7037(03)00451-4.

Hall, J. M., L. H. Chan, W. F. McDonough, and K. K. Turekian (2005), Determination of the lithium isotopic composition of planktic foraminifera and its application as a paleoseawater proxy, *Mar. Geol.*, *217*, 255–265, doi:10.1016/j.margeo.2004.11.015.

Hathorne, E., T. Felis, A. Suzuki, and H. Kawahata (2009), Lithium content of the aragonitic skeletons of massive *Porites* corals: A new tool to reconstruct tropical sea surface temperatures?, *Eos Trans. AGU*, *90*(52), Fall Meet. Suppl., Abstract PP34B-05.

Holcomb, M., A. L. Cohen, R. I. Gabitov, and J. L. Hutter (2009), Compositional and morphological features of aragonite precipitated experimentally from seawater and biogenically by corals, *Geochim. Cosmochim. Acta*, *73*, 4166–4179, doi:10.1016/j.gca.2009.04.015.

Huh, Y., L. H. Chan, L. Zhang, and J. M. Edmond (1998), Lithium and its isotopes in major world rivers: Implications for weathering and the oceanic budget, *Geochim. Cosmochim. Acta*, *62*, 2039–2051, doi:10.1016/S0016-7037(98)00126-4.

Kasemann, S. A., A. B. Jeffcoate, and T. Elliott (2005), Lithium isotope composition of basalt glass reference material, *Anal. Chem.*, *77*, 5251–5257, doi:10.1021/ac048178h.

Kasemann, S. A., D. N. Schmidt, J. Bijma, and G. L. Foster (2009), In situ boron isotope analysis in marine carbonates and its application for foraminifera and paleo-pH, *Chem. Geol.*, *260*, 138–147, doi:10.1016/j.chemgeo.2008.12.015.

Kinsman, D. J. J., and H. D. Holland (1969), The co-precipitation of cations with $CaCO_3$—IV. The co-precipitation of Sr^{2+} with aragonite between 16 and 96°C, *Geochim. Cosmochim. Acta*, *33*, 1–17, doi:10.1016/0016-7037(69)90089-1.

Kunioka, D., K. Shirai, N. Takahata, and Y. Sano (2006), Microdistribution of Mg/Ca, Sr/Ca, and Ba/Ca ratios in *Pulleniatina obliquiloculata* test by using a NanoSIMS: Implication for the vital effect mechanism, *Geochem. Geophys. Geosyst.*, *7*, Q12P20, doi:10.1029/2006GC001280.

Marriott, C. S., G. M. Henderson, N. S. Belshaw, and A. W. Tudhope (2004a), Temperature dependence of δ^7Li, δ^{44}Ca and Li/Ca during growth of calcium carbonate, *Earth Planet. Sci. Lett.*, *222*, 615–624, doi:10.1016/j.epsl.2004.02.031.

Marriott, C. S., G. M. Henderson, R. Crompton, M. Staubwasser, and S. Shaw (2004b), Effect of mineralogy, salinity, and temperature on Li/Ca and Li isotope composition of calcium carbonate, *Chem. Geol.*, *212*, 5–15, doi:10.1016/j.chemgeo.2004.08.002.

Meibom, A., J.-P. Cuif, F. Hillion, B. R. Constantz, A. Juillet-Leclerc, Y. Dauphin, T. Watanabe, and R. B. Dunbar (2004), Distribution of magnesium in coral skeleton, *Geophys. Res. Lett.*, *31*, L23306, doi:10.1029/2004GL021313.

Meibom, A., et al. (2006), Vital effects in coral skeletal composition display strict three-dimensional control, *Geophys. Res. Lett.*, *33*, L11608, doi:10.1029/2006GL025968.

Montagna, P., et al. (2009), Li/Mg ratios in shallow- and deep-sea coral exoskeletons as a new temperature proxy, *Eos Trans. AGU*, *90*(52), Fall Meet. Suppl., Abstract PP11A-1286.

Morozov, N. P. (1968), Geochemistry of rare alkaline elements in the oceans and seas, *Oceanology*, *8*, 169–178.

Pearce, N. J. G., W. T. Perkins, and J. A. Westgate (1997), A compilation of new and published major and trace element data for NIST SRM 610 and NIST SRM 612 Glass reference materials, *Geostand. Newsl.*, *21*, 115–144, doi:10.1111/j.1751-908X.1997.tb00538.x.

Rollion-Bard, C., N. Vigier, A. Meibom, D. Blamart, S. Reynaud, R. Rodolfo-Metalpa, S. Martin, and J. P. Gattuso (2009), Effect of environmental conditions and skeletal ultrastructure on the Li isotopic composition of scleractinian corals, *Earth Planet. Sci. Lett.*, *286*, 63–70, doi:10.1016/j.epsl.2009.06.015.

Ronov, A. B., A. A. Migdisov, N. T. Voskresenskaya, and G. A. Korzina (1970), Geochemistry of lithium in the sedimentary cycle, *Geochem. Int.*, *7*, 75–102.

Rosner, M., W. Bach, H. Paulick, and J. Erzinger (2004), Lithium and strontium isotope compositions of serpentinite-hosted carbonate veins from the MAR (ODP Leg 209), Records of different stages of seafloor metamorphism, *Eos Trans. AGU*, *85*(47), Fall Meet. Suppl., Abstract V23B-0626.

Rosner, M., L. Ball, B. Peucker-Ehrenbrink, J. Blusztajn, W. Bach, and J. Erzinger (2007), A simplified, accurate and fast method for lithium isotope analysis of rocks and fluids, and delta Li-7 values of seawater and rock reference materials, *Geostand. Geoanal. Res*, *31*, 77–88, doi:10.1111/j.1751-908X.2007.00843.x.

Rosner, M., M. Wiedenbeck, and T. Ludwig (2008), Composition-induced variations in SIMS instrumental mass fractionation during boron isotope ratio measurements of silicate glasses, *Geostand. Geoanal. Res.*, *32*, 27–38, doi:10.1111/j.1751-908X.2008.00875.x.

Sano, Y., K. Shirai, N. Takahata, T. Hirata, and N. C. Sturchio (2005), Nano-SIMS analysis of Mg, Sr, Ba and U in natural calcium carbonate, *Anal. Sci.*, *21*, 1091–1097, doi:10.2116/analsci.21.1091.

Shaheen, M., J. E. Gagnon, Z. Yang, and B. J. Fryer (2008), Evaluation of the analytical performance of femtosecond laser ablation inductively coupled plasma mass spectrometry at 785 nm with glass reference materials, *J. Anal. At. Spectrom.*, *23*, 1610–1621, doi:10.1039/b809880h.

Shirai, K., M. Kusakabe, S. Nakai, T. Ishii, T. Watanabe, H. Hiyagon, and Y. Sano (2005), Deep-sea coral geochemistry: Implication for the vital effect, *Chem. Geol.*, *224*, 212–222, doi:10.1016/j.chemgeo.2005.08.009.

Shirai, K., T. Kawashima, K. Sowa, T. Watanabe, T. Nakamori, N. Takahata, H. Amakawa, and Y. Sano (2008), Minor and trace element incorporation into branching coral *Acropora nobilis* skeleton, *Geochim. Cosmochim. Acta*, *72*, 5386–5400, doi:10.1016/j.gca.2008.07.026.

Sinclair, D. J., B. Williams, and M. Risk (2006), A biological origin for climate signals in corals—Trace element "vital effects" are ubiquitous in Scleractinian coral skeletons, *Geophys. Res. Lett.*, *33*, L17707, doi:10.1029/2006GL027183.

Tomascak, P. B. (2004), *Geochemistry of Non-Traditional Stable Isotopes, Rev. Mineral. Geochem.*, vol. 55, 166 pp., edited by C. M. Johnson, B. L. Beard, and F. Albarede, Mineral. Soc. of Am., Washington, D. C.

Vigier, N., C. Rollion-Bard, S. Spezzaferri, and F. Brunet (2007), In situ measurements of Li isotopes in foraminifera, *Geochem. Geophys. Geosyst.*, *8*, Q01003, doi:10.1029/2006GC001432.

Watson, E. B. (1996), Surface enrichment and trace-element uptake during crystal growth, *Geochim. Cosmochim. Acta*, *60*, 5013–5020, doi:10.1016/S0016-7037(96)00299-2.

Watson, E. B. (2004), A conceptual model for near-surface kinetic controls on the trace-element and stable isotope composition of abiogenic calcite crystals, *Geochim. Cosmochim. Acta*, *68*, 1473–1488, doi:10.1016/j.gca.2003.10.003.

Watson, E. B., and Y. Liang (1995), A simple model for sector zoning in slowly growing crystals: Implications for growth rate and lattice diffusion, with emphasis on accessory minerals in crustal rocks, *Am. Mineral.*, *80*, 1179–1187.

White, W. M. (2005), Stable isotope geochemistry, in *Geochemistry: An Online Text Book* [electronic], Johns Hopkins Univ. Press, Baltimore, Md. (Available at http://www.imwa.info/geochemistry/Chapters/Chapter09.pdf)